Contribution from the Department of Chemistry,
University of Kansas, Lawrence, Kansas 66045

Crystal and Molecular Structure of Trihydrogen Diethylenetriaminepentaacetatocuprate(II) Monohydrate ($H_3CuDTPA \cdot H_2O$)

R. C. SECCOMBE, B. LEE,* and G. M. HENRY

Received October 9, 1974 AIC40697B

The title compound crystallizes in the triclinic space group $P\bar{1}$ with the following cell dimensions: a = 6.443 (2) Å, b = 9.524 (4) Å, c = 16.308 (8) Å, α = 101.20 (4)°, β = 93.89 (4)°, γ = 104.51 (3)°. There are two molecules in a unit cell. The structure was determined from 5326 three-dimensional X-ray diffraction data collected on an automatic four-circle diffractometer by the θ–2θ scan technique using Mo Kα radiation up to a 2θ angle of 65°. It was refined by the least-squares procedure to the conventional R value of 0.035. The crystal consists of discrete complexes connected together by a network of hydrogen bonds. One water molecule per complex participates in this hydrogen-bond network. The complex may be described as a sexadentate, six-coordinate species. Two of the chelated ligands are oxygen atoms of the carboxyl groups from each end of the molecule. The average Cu–O distance is 1.974 (4) Å. Another two are the central nitrogen atom and a terminal nitrogen atom. The average Cu–N distance is 2.049 (7) Å. These four atoms lie roughly at the corners of a square. The remaining two ligands are much more weakly bound. These are a nitrogen atom at a distance of 2.366 (2) Å from the metal ion and an oxygen atom of the central carboxyl group at 2.518 (2) Å. The central and the two uncoordinated carboxyl groups carry the three acid protons.

Introduction

Diethylenetriaminepentaacetic acid (DTPA) is a strong

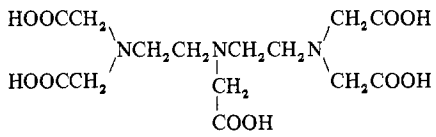

chelating agent.[1] Structures for several of the metal complexes formed with DTPA have been suggested on the basis of potentiometric titration, infrared spectroscopic, and proton magnetic resonance studies.[2-5] A single-crystal X-ray structure determination of the nine-coordinate neodymium complex has been reported.[6] This paper describes a detailed X-ray crystal structure determination of the trihydrogen copper(II) complex. Preliminary results of this work have been presented elsewhere.[7] Since then a short communication on the crystal structure work of this complex appeared in the literature.[8] These workers' results are, however, significantly different from those reported herein.

Experimental Section

Crystal Data. The large, blue, needle-shaped crystals of $H_3Cu^{II}DTPA \cdot H_2O$ were prepared and kindly supplied to us by Dr. Sievers.[3] A number of Weissenberg and precession photographs taken of these crystals indicated that the crystals were triclinic with two molecules per unit cell. The space group was thus assumed to be $P\bar{1}$ and this assignment was later confirmed by the successful determination of the full structure. Accurate cell dimensions were determined by a least-squares fit of the orientation angles of some 15 reflections measured on a Syntex $P\bar{1}$ four-circle diffractometer using Zr-filtered Mo Kα radiation. The reflections chosen were widely spread in the reciprocal space with the 2θ angles in the range of 11–32°. The density of the crystal was measured by flotation in petroleum ether and tetrabromoethane. Some of the crystal data are summarized here for empirical formula $CuC_{14}H_{23}N_2O_{11}$: mol wt 472.89, space group $P\bar{1}$, a = 6.443 (2) Å, b = 9.524 (4) Å, c = 16.308 (8) Å, α = 101.20 (4)°, β = 93.89 (4)°, γ = 104.51 (3)°, Z = 2, d_{obsd} = 1.69 g/cm^3, d_{calcd} = 1.665 g/cm^3, $F(000)$ = 490, λ(Mo Kα) 0.710688 Å, μ(Mo Kα) = 12.7 cm^{-1}.

Intensity Data Collection. A parallelepiped-shaped crystal with approximate dimensions of 0.20 × 0.18 × 0.15 mm was mounted in random orientation on a Syntex $P\bar{1}$ computer-controlled four-circle diffractometer equipped with a scintillation counter and a pulse height analyzer. Zr-filtered Mo Kα radiation was used with a takeoff angle of 2°. Intensities were collected by a θ–2θ scan technique. The scan rate was varied between 1 and 24° min^{-1} depending upon the intensity of the reflection. The scan range was from 1° below the 2θ angle for the Kα_1 component to 1° above that for the Kα_2 component. Background intensity was measured for each reflection by counting for half the total scan time at each end of the scan range. A set of five "standard" reflections, selected to represent different ranges of intensity and different regions in reciprocal space, were measured after every 100 reflections. The data were collected in concentric shells in reciprocal space with the 2θ ranges 0–45, 45–55, 55–60, and 60–65°. Intensities of a total of 6833 independent reflections were measured in this manner.

It was found that spikes of high count and short duration occurred a number of times during data collection. The cause of these spikes was not determined. A total of 18 reflections were found to be affected by these spikes and were either remeasured or eliminated from the data set.

When intensities fell between 10,000 and 40,000 counts sec^{-1}, coincidence correction was made using the formula $I_t = I_0 + \tau I_t^2$, which is an approximation to the formula[9,10] $I_t = I_0 \exp(I_t\tau)$ where I_t is the corrected count, I_0 is the raw uncorrected count, and τ is the counter circuit dead time. An estimated value of 1.68×10^{-6} sec was used for τ. Two reflections were found to have an intensity higher than 40,000 counts sec^{-1}. These were measured again at a lower tube current setting.

The integrated intensity, I, and its estimated variance σI^2 were obtained for each reflection using the expressions $I = r[S - (t_s/t_b)(B_1 + B_2)]$ and $\sigma I^2 = r^2[S + (t_s/t_b)^2(B_1 + B_2)]$ where r is the scan rate in degrees per minute, S is the scan count, t_s and t_b are the durations in times taken for the scan and the background counts (t_s/t_b = 1 in this case), and B_1 and B_2 are the left and right background counts. The intensities of the "standard" reflections decreased steadily during the data collection. The total decrease amounted to about 8%. The body of the data was scaled accordingly. After the scaling the root-mean-square deviation of the "standard" reflections was 2.5%. The variance of the intensity was also scaled and then increased by $(pI)^2$ after the manner of Corfield, *et al.*[11] The value of p was chosen to be 0.03, which was the relative rms deviation of the "standard" reflections.

For the entire structure analysis that followed, only those reflections with $I \geq 3\sigma I$ were used. There were 5326 such reflections. The intensity data were converted to the structure factors through the application of the Lorentz–polarization factor in its usual form. No absorption or extinction correction was applied. A maximum error of about 6% in intensity is to be expected from the neglect of the absorption effect.

Structure Determination and Refinement. The structure was determined by an application of the heavy-atom technique. It was refined by the least-squares procedures which minimized the function $\sum w(|F_o| - |F_c|)^2$. The weight w was chosen to be $1/\sigma F^2 = 4LpI/\sigma I^2$ where Lp is the Lorentz–polarization factor.

Initially only the nonhydrogen atoms were identified. After several cycles of isotropic refinement all hydrogen atoms could be seen clearly in a difference electron density map. All carbon-attached hydrogen atom positions were then calculated using a C–H distance of 0.95 Å. These hydrogen atoms were included in subsequent refinements, fixed at their calculated positions with isotropic thermal parameters

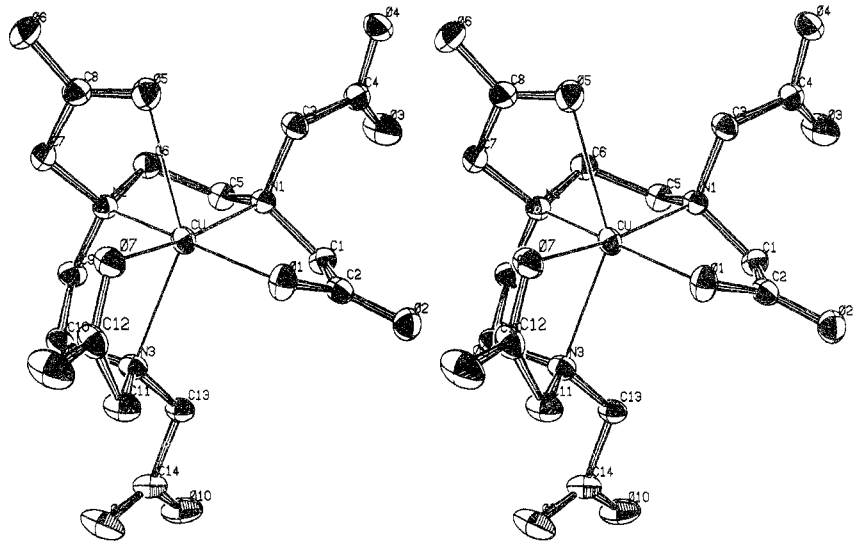

Figure 1. Stereoscopic view of the complex.

that were 10% larger than those of the carbon atoms to which they were attached. All nonhydrogen atoms were treated anisotropically and the anomalous dispersion effect of copper was included. The discrepancy indices R and R' ($=\sum w(|F_o| - |F_c|)^2/\sum w|F_o|^2$) were 0.039 and 0.049, respectively, at the end of this procedure. The estimated standard deviation of an observation of unit weight, $\sigma = [\sum w(|F_o| - |F_c|)^2/(n-p)]^{1/2}$, where $n = 5326$ and $p = 262$, was 1.90.

Two more cycles of least squares were carried out in order to refine the hydrogen positions. In these cycles only the overall scale factor, the positional parameters of the carbon-attached hydrogens, and the positional and isotropic thermal parameters of the oxygen-attached hydrogens were allowed to vary. The isotropic thermal parameters of the carbon-attached hydrogens were fixed to be equal to the isotropic equivalents of the anisotropic thermal parameters of the carbon atoms to which they were attached. The final discrepancy indices after this refinement were 0.036 and 0.044, respectively, for R and R'. The final difference map showed residual features reaching ±0.3 e/Å^3 except near the position of copper where a peak and a valley of 0.4 e/Å^3 and −0.5 e/Å^3 remained.

Computer programs used for the cell dimension measurement and data collection were supplied by Syntex Analytical Instruments. The main crystallographic computations were carried out using the Honeywell 635 computer at the University of Kansas. Local versions of some well-known programs[12] were used as well as others that were locally developed. The atomic scattering factors used were from Cromer and Mann's[13] tables for Cu^{2+}, O, N, and C and from Ibers'[14] tables for H and for anomalous factors of Cu.

The observed and calculated structure factors are given in Table I.[15] The final structural parameters from which the structure factors of Table I were calculated are given in Tables II[15] and III.

Results and Discussion

Overall Structure. The crystal consists of a racemic mixture of discrete complex molecules connected to one another by hydrogen bonds. A stereodrawing of the molecule that shows the numbering scheme used for the atoms is given in Figure 1. The complex is sexadentate and two carboxyl groups, one from each terminal nitrogen, remain uncoordinated. The three acid protons required by stoichiometry to be on the complex are carried, one each, on the loosely bound (see below) central carboxyl group and the uncoordinated groups. More specifically, these hydrogens are attached to O4, O6, and O10 atoms.

Bond lengths in the discrete complex molecule are given in Table IV. The C–C and C–N distances average to 1.524 and 1.485 Å, respectively, and are similar to those found in EDTA complexes.[16] The C–O distances show an interesting variation. The two C–O bonds in a carboxyl group are very different in two cases (those involving C4 and C14) in which the carboxyl group is not bonded to the metal ion but carries a proton. On the other hand they are similar in two other cases (those involving C2 and C12) in which the carboxyl group is bonded to the metal ion and not protonated. In these cases the C–O bond that involves the coordinated oxygen is somewhat longer than the other. An intermediate pattern is observed in the two

Table III. Positional and Isotropic Thermal Parameters[a]

	10^4x	10^4y	10^4z	B,[b] Å^2
Cu	2109.7 (4)	1576.7 (3)	2516.5 (2)	1.545 (6)
O_1	4674 (2)	2787 (2)	3311 (1)	2.07 (4)
O_2	5823 (3)	3571 (2)	4677 (1)	2.21 (4)
O_3	2000 (3)	−1144 (2)	4799 (1)	3.40 (5)
O_4	3923 (3)	−2397 (2)	4003 (1)	2.67 (4)
O_5	2607 (3)	−758 (2)	1620 (1)	2.33 (4)
O_6	1124 (3)	−1972 (2)	315 (1)	3.53 (5)
O_7	3241 (2)	2404 (2)	1568 (1)	1.98 (4)
O_8	4355 (3)	4450 (2)	1082 (1)	3.08 (5)
O_9	−913 (3)	6239 (2)	2822 (1)	3.52 (5)
O_{10}	−2116 (3)	5827 (2)	4009 (1)	3.14 (5)
O_W[c]	4237 (3)	6833 (2)	328 (1)	3.64 (6)
N_1	1554 (3)	504 (2)	3492 (1)	1.55 (4)
N_2	−873 (3)	322 (2)	1942 (1)	1.66 (4)
N_3	541 (3)	3573 (2)	2521 (1)	1.70 (4)
C_1	2408 (3)	1724 (2)	4253 (1)	1.81 (5)
C_2	4460 (3)	2765 (2)	4076 (1)	1.73 (4)
C_3	2809 (3)	−609 (2)	3440 (1)	1.82 (5)
C_4	2820 (3)	−1390 (2)	4169 (1)	1.95 (5)
C_5	−832 (3)	−182 (2)	3378 (1)	1.90 (5)
C_6	−1615 (3)	−827 (2)	2445 (1)	1.94 (5)
C_7	−738 (4)	−414 (2)	1065 (1)	2.10 (5)
C_8	1184 (4)	−1065 (2)	1033 (1)	2.10 (5)
C_9	−2391 (3)	1284 (2)	1949 (1)	2.03 (5)
C_{10}	−1297 (3)	2840 (2)	1853 (1)	1.99 (5)
C_{11}	2275 (4)	4614 (2)	2223 (1)	2.19 (5)
C_{12}	3368 (3)	3765 (2)	1570 (1)	1.97 (5)
C_{13}	−101 (3)	4201 (3)	3324 (1)	1.82 (5)
C_{14}	−1102 (3)	5496 (2)	3338 (1)	2.21 (5)
$H(O_4)$[d]	3953 (54)	−2877 (38)	4392 (21)	3.17 (75)
$H(O_6)$[d]	2316 (64)	−2322 (44)	353 (26)	4.62 (92)
$H(O_{10})$[d]	−2635 (52)	5069 (36)	4259 (20)	2.62 (69)
$H_1(O_W)$[d]	4405 (65)	6396 (43)	−139 (26)	4.45 (91)
$H_2(O_W)$[d]	4197 (54)	6143 (36)	650 (22)	2.82 (71)

[a] Estimated standard deviations referred to the least significant digit are given in parentheses throughout this paper. [b] The isotropic thermal parameters for nonhydrogen atoms were derived from the refined anisotropic thermal parameters using the formula $B = (4/3)(\beta_{11}g_{11} + \beta_{22}g_{22} + \beta_{33}g_{33} + 2\beta_{12}g_{12} + 2\beta_{13}g_{13} + 2\beta_{23}g_{23})$ where g's are the elements of the metric tensor and β's give the anisotropic temperature factor in the form of $\exp[-(\beta_{11}h^2 + \beta_{22}k^2 + \beta_{33}l^2 + 2\beta_{12}hk + 2\beta_{13}hl + 2\beta_{23}kl)]$. [c] This is the oxygen atom of the water molecule of hydration. [d] These are hydrogen atoms attached to the oxygen atoms given in the parentheses.

Table IV. Bond Lengths (Å)

Cu-N_1	2.056 (2)	C_1-C_2	1.523 (3)
Cu-N_2	2.042 (2)	C_3-C_4	1.521 (3)
Cu-N_3	2.366 (2)	C_5-C_6	1.524 (3)
Cu-O_1	1.978 (2)	C_7-C_8	1.517 (3)
Cu-O_5	2.518 (2)	C_9-C_{10}	1.517 (3)
Cu-O_7	1.970 (2)	C_{11}-C_{12}	1.528 (3)
C_2-O_1	1.269 (2)	C_{13}-C_{14}	1.525 (3)
C_2-O_2	1.254 (3)	N_1-C_1	1.490 (3)
C_4-O_3	1.195 (3)	N_1-C_3	1.479 (3)
C_4-O_4	1.329 (3)	N_1-C_5	1.495 (3)
C_8-O_5	1.217 (3)	N_2-C_6	1.497 (3)
C_8-O_6	1.305 (3)	N_2-C_7	1.483 (3)
C_{12}-O_7	1.278 (3)	N_2-C_9	1.498 (3)
C_{12}-O_8	1.236 (3)	N_3-C_{10}	1.481 (3)
C_{14}-O_9	1.194 (3)	N_3-C_{11}	1.474 (3)
C_{14}-O_{10}	1.337 (3)	N_3-C_{13}	1.461 (3)

Table V. Bond Angles (deg)

CuN_1C_1	103.05 (12)	$C_1N_1C_3$	110.49 (16)
CuN_1C_3	109.04 (12)	$C_3N_1C_5$	112.87 (16)
CuN_1C_5	105.00 (12)	$C_5N_1C_1$	115.58 (16)
CuN_2C_6	106.23 (12)	$C_6N_2C_7$	109.83 (16)
CuN_2C_7	110.46 (13)	$C_7N_2C_9$	110.42 (16)
CuN_2C_9	109.67 (12)	$C_9N_2C_6$	110.13 (16)
CuN_3C_{10}	99.51 (12)	$C_{10}N_3C_{11}$	111.77 (17)
CuN_3C_{11}	100.14 (12)	$C_{11}N_3C_{13}$	114.08 (17)
CuN_3C_{13}	116.08 (12)	$C_{13}N_3C_{10}$	113.69 (16)
$N_1C_1C_2$	108.66 (16)	$C_1C_2O_1$	116.98 (18)
$N_1C_3C_4$	116.77 (16)	$C_3C_4O_3$	126.46 (19)
$N_1C_5C_6$	109.50 (16)	$C_7C_8O_5$	122.68 (19)
$N_2C_6C_5$	110.36 (16)	$C_{11}C_{12}O_7$	118.49 (17)
$N_2C_7C_8$	110.50 (17)	$C_{13}C_{14}O_9$	123.75 (20)
$N_2C_9C_{10}$	112.85 (16)	$C_1C_2O_2$	119.88 (18)
$N_3C_{10}C_9$	110.94 (16)	$C_3C_4O_4$	108.90 (17)
$N_3C_{11}C_{12}$	110.46 (17)	$C_7C_8O_6$	112.55 (19)
$N_3C_{13}C_{14}$	116.71 (17)	$C_{11}C_{12}O_8$	117.64 (19)
CuO_1C_2	113.80 (13)	$C_{13}C_{14}O_{10}$	115.39 (19)
CuO_5C_8	103.24 (13)	$O_1C_2O_2$	123.12 (19)
CuO_7C_{12}	118.99 (13)	$O_3C_4O_4$	124.64 (19)
N_1CuN_2	87.45 (8)	$O_5C_8O_6$	124.77 (20)
N_2CuN_3	83.35 (7)	$O_7C_{12}O_8$	123.87 (19)
N_1CuO_1	81.91 (7)	$O_9C_{14}O_{10}$	120.71 (20)
N_2CuO_5	72.76 (7)	N_3CuO_1	94.36 (7)
N_3CuO_7	76.79 (7)	N_3CuN_1	116.03 (7)
N_1CuO_7	166.25 (6)	O_5CuO_1	114.65 (7)
N_2CuO_1	166.85 (6)	O_5CuN_1	89.53 (7)
N_3CuO_5	144.28 (6)	O_5CuO_7	81.34 (7)
		O_7CuO_1	92.52 (7)
		O_7CuN_2	99.52 (8)

C–O bonds of the fifth carboxyl group (one that contains C_8) wherein one oxygen is protonated while the other is bonded to the metal ion.

The bond angles are given in Table V. They show considerable variations from the expected ideal values. Discussion of these angles is given in the Appendix where the conformation of the chelating agent is described in detail.

The complex molecule contains five five-membered chelate rings that are contiguously joined and fused together. In this paper the following labels will be used for these five chelate rings. E1 and E2 are the two ethylenediamine rings (E rings) that contain atoms N_1 and N_3, respectively. G1, G2, and G3 are the three glycinate rings (G rings) that contain atoms O_1, O_5, and O_7, respectively. All of these rings are highly ruffled. The ruffling of a five-membered chelate ring may be described by means of two dihedral angles ϕ_1 and ϕ_2.[16] The ring is called δ or λ type depending on whether the angle $\phi_{21} = \phi_2 - \phi_1$ is positive or negative.[16,17] The overall degree of ruffling may be measured by $|\phi_1| + |\phi_2|$[16] or by the ring angle sum.[18,19] (The ring type designation and the values of ϕ_1, ϕ_2, and ring angle sum are given later in Table VIII.) A detailed discussion of the conformation of the ring system is given in the Appendix.

Coordination Geometry. The coordination geometry may be described in terms of a highly irregular octahedron of which the dimensions are given in Table VI. Two nitrogen atoms, N_1 and N_2, and two oxygen atoms, O_1 and O_7, form relatively strong bonds to the metal ion. The average Cu–N and Cu–O distances are 2.049 (7) and 1.974 (4) Å, respectively (Table IV). Roughly speaking, these four atoms are at the corners of a square. The plane of the square is, however, poorly defined—the rms deviation of the four atoms from the least-squares plane through them is 0.16 Å. The metal ion lies 0.05 Å off this plane. The substantial deviation of these four atoms from an ideal square can also be seen readily from the dimensions given in Table VI.

Table VI. Coordination Polyhedron Edge Lengths (Å)

O_5-O_1	3.796 (3)	N_3-O_1	3.197 (3)
O_5-N_1	3.238 (3)	N_3-N_1	3.754 (3)
O_5-N_2	2.732 (2)	N_3-N_2	2.941 (3)
O_5-O_7	2.954 (3)	N_3-O_7	2.711 (2)
O_1-N_1	2.645 (2)	N_2-O_7	3.063 (3)
N_1-N_2	2.833 (3)	O_7-O_1	2.852 (3)

The axial ligands, N_3 and O_5, are much more weakly bound. The Cu–N_3 distance is more than 0.3 Å longer than the other two Cu–N distances (Table IV) while the Cu–O_5 distance is even longer than the Cu–N_3 distance. These atoms are also considerably off from the main axis of the coordination polyhedron. If one defines this axis as the one that passes the equatorial plane (the mean plane of the atoms O_1, N_1, N_2, and O_7) perpendicularly at the metal ion, atoms N_3 and O_5 are off from this axis by 0.82 and 0.91 Å, respectively, and the Cu–N_3 and Cu–O_5 bonds make angles of 20 and 21° to the main axis. The large deviations of the N_3CuO_5 angle from 180° and of the N_3CuN_1 and O_5CuO_1 angles from 90° can also be noted (Table V).

A d^9 Cu(II) complex is subject to the Jahn–Teller effect[20] and the cited distortions are probably in part due to this effect. One should, however, note the strongly noncentrosymmetric nature of the distortion. It is clear that the overriding force for the distortion in this system derives from the many interatomic repulsions among the crowded atoms of the chelating agent and from the geometric constraints attendant on the formation of a system of the five fused, contiguously joined chelate rings. A detailed description of the geometrical aspects of the chelating agent, including an enumeration of all possible geometrical and conformational isomers, is given in the Appendix.

Relation to Other Physicochemical Properties. The potentiometric titration behavior of the 1:1 Cu–DTPA complex[2,21] shows that three of the five acid protons of DTPA dissociate immediately upon complexation. The remaining two dissociate less readily with different pK values. The observed crystalline structure of the complex is consistent with this behavior and suggests that the two titratable protons in the dihydrogen species are attached to the two uncoordinated free carboxylic acid arms. The two protons have slightly different dissociation constants because one of the carboxyl groups is attached to a strongly bonded nitrogen while the other is attached to a weakly bonded nitrogen and is farther away from the equatorial plane of the complex.

On the other hand, in view of the large number of isomers possible (see Appendix), it should not be assumed that the observed crystalline structure represents the only significant species in solution. Indeed the structural models of the nitrocobalt(III) complex of DTPA from proton magnetic resonance studies[4,22] may be derived from entirely different isomer types (types I and V in Figure 3). Thus the possibility remains at present that more than one isomer of comparable stability coexist in solution in a dynamic equilibrium.

In this connection, it is interesting to compare this structure with that of the same molecule reported by Fomenko and his

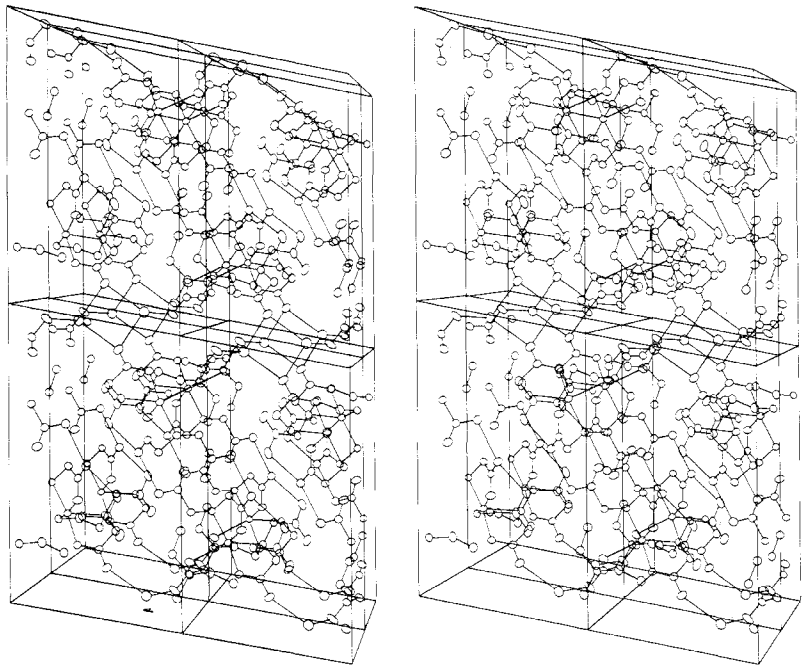

Figure 2. Stereoscopic view of the molecular packing in the crystal. Four complete unit cells are shown. The crystallographic *a* axis is roughly along the viewing direction, the *b* axis is horizontal, and the *c* axis is vertical.

coworkers.[8] Although it is not possible to obtain a full picture of their structure from the published short communication, it is clear that theirs is different from the structure reported herein. Their crystal is also triclinic but has different unit cell dimensions and a different density. Their structure is also formally sexadentate wherein the three nitrogens and the three acetate groups, one from each nitrogen, are bonded to the metal ion. However, the equatorial coordination plane of their structure contains two terminal nitrogens rather than a terminal nitrogen and the middle nitrogen as in our structure. Their coordination bond lengths are also substantially different from those of ours. More detailed comparison of the two structures must wait until a more complete account of the Russian workers' structure is available.

The fully ionized form of the DTPA complexes of Fe(II), Co(II), Ni(II), Cu(II), Zn(II), and Cd(II) have stability constants[23] that are about 2 units higher than those of the corresponding EDTA complexes.[2a] This is primarily because a fully ionized DTPA molecule carries one more negative charge and thus interacts more strongly with a metal ion than a fully ionized EDTA.[2a] When the stability constants of the monohydrogen species of DTPA complexes are compared with those of the fully ionized EDTA complexes, one finds that the former are about 3 units smaller than the latter.[2a] If this trend is extrapolated to the neutral species, one expects the trihydrogen copper(II) complex of DTPA to be less stable than the dihydrogen copper(II) complex of EDTA. The structure of the H_3Cu^{II}–DTPA complex may be compared in this light with that of the H_2Cu^{II}–EDTA–H_2O complex.[24]

One finds that the strength of the coordination bonds in the DTPA complex is about equal to or much weaker than that in the EDTA complex. Ring strain as measured by the ring angle sum is significantly less in the EDTA complex (see Appendix). The overall impression is that a DTPA molecule finds it more awkward to wrap around the metal ion than EDTA does. The enthalpic contribution to the stability of the Cu^{II}–DTPA complex is, therefore, likely to be less than that for the Cu^{II}–EDTA complex of equal charge.

The situation with regard to entropy is more murky. A free DTPA molecule has more degrees of freedom than a free EDTA molecule and may be expected to lose more entropy upon complex formation. On the other hand, judging from the observed crystalline structures, the DTPA complex has a more "loose" structure than the corresponding EDTA complex. Another source of uncertainty is in the number of water molecules that are associated with a free metal ion in solution but freed upon complex formation. In the acidic EDTA complex one water molecule remains bound to the metal ion. The observed acidic DTPA complex does not have a water molecule directly bonded to the metal ion. If this feature persists in solution, the entropy of formation of the DTPA complex will be larger than that of the EDTA complex by an amount corresponding to the liberation of a coordinated water molecule. However, in view of the extremely weak nature of the Cu–O_5 bond, it is not clear whether this bond remains intact in solution. The evidence from the infrared spectrum is inconclusive[3] although the fact that it differs from that of the trihydrogen nickel(II) complex of DTPA may be significant.

Molecular Packing. The basic unit of the molecular packing arrangement may be considered to be an infinite chain of molecules, the axis of which runs parallel to the *a* axis and passes through the point 0, 0, $^1/_2$. It is one molecule thick roughly along the [021] direction and two molecules thick roughly along the [02$\bar{3}$] direction (Figure 2). Two molecules in this chain, related to one another by a center of inversion at $^1/_2$, 0, $^1/_2$, are linked together by two hydrogen bonds which connect the O_2 atom of one molecule to the O_4 atom of the other. The infinite chain is generated from this two-molecule unit by simple cell translation along the *a* axis. Two units related by cell translation are connected together by two hydrogen bonds, each connecting the O_2 atom of one molecule to the O_{10} atom of the other related by the cell translation.

The entire crystal consists of this basic chain repeated throughout the crystal by simple cell translations along the *b* and *c* directions. Four of these chains are linked by a curious square array of hydrogen bonds centered at the crystallographic center of inversion symmetry element at $^1/_2$, $^1/_2$, 0. One water molecule is hydrogen bonded to the O_8 atom of one chain, to another O_8 atom of a second chain related to the first by the inversion symmetry, and to the O_6 atom of a third chain related to the first one by the *b* cell translation. The two hydrogen atoms of the water molecule are directed toward the two O_8 atoms while the hydrogen attached to the O_6 atom is directed

Table VII

a. Bond Lengths and Angles Involving Oxygen-Attached Hydrogen Atoms[a]

	Lengths, Å		
O_4-H(O_4)	0.85 (3)	H(O_4)-O_2'	1.78 (3)
O_6-H(O_6)	0.91 (4)	H(O_6)-O_W'	1.64 (4)
O_{10}-H(O_{10})	0.90 (3)	H(O_{10})-O_2'	1.80 (3)
O_W-H_1(O_W)	0.91 (3)	H_1(O_W)-O_8'	1.90 (3)
O_W-H_2(O_W)	0.82 (4)	H_2(O_W)-O_8'	1.91 (4)
	Angles, Deg		
C_4-O_4-H(O_4)	112 (2)	O_4-H(O_4)-O_2'	170 (3)
C_8-O_6-H(O_6)	107 (3)	O_6-H(O_6)-O_W'	172 (4)
C_{14}-O_{10}-H(O_{10})	115 (2)	O_{10}-H(O_{10})-O_2'	169 (3)
H_1(O_W)-O_W-H_2(O_W)	103 (3)	O_W-H_1(O_W)-O_8'	166 (3)
		O_W-H_2(O_W)-O_8'	163 (4)

b. Hydrogen Bond Lengths and Angles[a]

	Lengths, Å		
O_4-O_2'	2.626 (2)	O_W-O_8	2.798 (3)
O_6-O_W'	2.543 (3)	O_W-O_8'	2.711 (3)
O_{10}-O_2'	2.691 (3)		
	Angles, Deg		
C_4'-O_4'-O_2	108.1 (1)	C_{12}-O_8-O_W	139.2 (1)
C_8'-O_6'-O_W	111.4 (2)	C_{12}-O_8-O_W'	124.7 (2)
C_{14}'-O_{10}'-O_2	117.7 (1)	O_W-O_8-O_W'	88.3 (1)
C_2-O_2-O_4'	114.4 (1)	O_6'-O_W-O_8	124.6 (1)
C_2-O_2-O_{10}'	102.9 (1)	O_6'-O_W-O_8''	123.9 (1)
O_4'-O_2-O_{10}''	141.9 (1)	O_8-O_W-O_8'	91.7 (1)

[a] Primes are used to distinguish atoms in different molecules.

to the water molecule. Another water molecule related to this one by the inversion symmetry forms an equivalent set of hydrogen bonds to complete the square network. Dimensions of these and other hydrogen bonds are given in Table VII.

Acknowledgment. We thank Dr. Robert E. Sievers for providing us with crystals used in this study and Professor J. L. Hoard in whose laboratory the crystallographic study of this compound was initiated. This work was supported by the National Institutes of Health through the Health Science Advancement Award and by the University of Kansas General Research Fund.

Appendix

Isomerism. Seven types of topological isomers must be considered for a sexadentate octahedral metal complex of DTPA (Figure 3). Each contains two E rings, three G rings, and two uncomplexed free carboxylic acid arms. The isomers in which a nitrogen atom is not coordinated are excluded, as are those in which a ring spans a trans pair of ligands. More than one conformational isomer exist for each type (see below). Each one is optically active and only one of the optical pair is being considered for each type. The observed structure corresponds to type VII.

All possible conformational isomers can be derived for each of these topological types by considering possible conformations of an isolated five-membered ring and then considering possible ways of fusing these rings pairwise.

A general nonplanar five-membered ring can assume four different conformations—a generalized envelope form and its mirror image and a generalized half-chair form and its mirror image.[16] These correspond to different sign combinations of the angles ϕ_1 and ϕ_2. For E rings, only the two half-chair forms need be considered (ϕ_1 and ϕ_2 have opposite signs; see Table VIII). For G rings, all four forms can and do occur. However, for the purpose of delineating the gross shape of the molecule, the four ring atoms C–C–O–M, where M is the metal ion, may be assumed to lie in one plane. (This is equivalent to assuming ϕ_2 to be negligible. Values given in ref 16 and in Table VIII show that ϕ_2 is indeed small.) Only two different conformational types may then be recognized for a G ring also.[16]

There are two fundamentally different ways of fusing one ring to an E ring. One leads to an *S* and the other to an *R* configuration around the tetrahedral nitrogen at the ring juncture. The standard rules used for the *S*–*R* designation,[25] however, can lead to confusion because two of the groups attached to the nitrogen often have the same numbering hierarchy or one that depends on the conformation of other remote parts of the molecule. Fortunately, the substantial pucker of the E ring makes it possible to use the equatorial–axial classification. Any group attached to an E ring will be called equatorial or axial depending on whether the carbon atom of the group bonded to the nitrogen is equatorial or axial with respect to the E ring.

When the various E- and G-ring types are fused to an E ring using these two modes of attachment, it is found that seven distinct types of ring pairs are possible (Figure 4).[26]

The disposition of the three ligand atoms of a ring pair varies notably among these different types. Some are suitable for a cis coordination while others will prefer a trans arrangement. A measure of these preferences may be obtained from the angle between the mean planes of the two ring planes or that between the planes of the ligand atoms. One sample set of these values is given in Table IX.[27] Although these values can vary considerably in different situations, it is nonetheless clear that all but one ring pair have one definitely preferred configuration as indicated in the last column of Table IX.[28]

The whole sexadentate, octahedral complex may be assembled using these different ring-pair types with proper attention given to their preferred configuration. When this is done, the following number of conformational isomers are

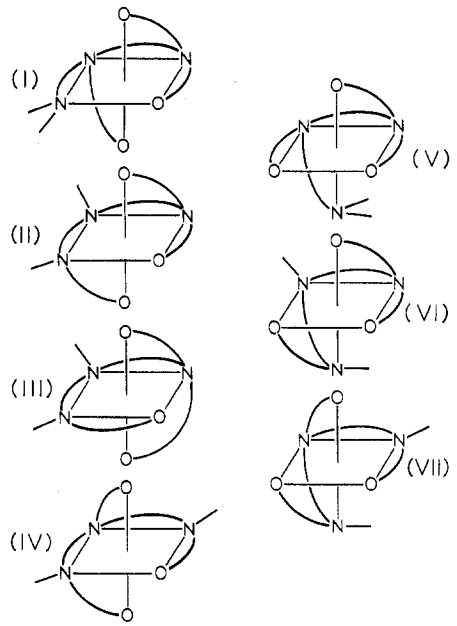

Figure 3. Schematic diagrams of the seven possible topological isomer types.

Table VIII. Ring Conformation Angles

	ϕ_1,[a] deg	ϕ_2,[a] deg	Type[b]	Ring angle sum, deg
E1	28	−24	λ	518
E2	23	−34	λ	517
G1	−28	−4	δ	525
G2	28	15	λ	520
G3	29	7	λ	525

[a] The angles ϕ_1 and ϕ_2 are defined in ref 16. Atom B1 in Figure 1 of that reference is taken to be N_1 for the E1 ring, N_2 for the E2 ring, and the nitrogen atom for the G rings. The angles given are for the optical isomer shown in Figure 1 of this paper. The sign of all the angles must be changed for the enantiomer. [b] The types given are for the optical isomer shown in Figure 1.

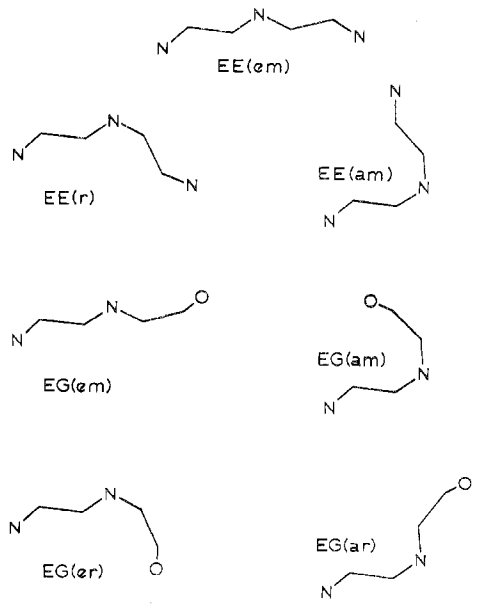

Figure 4. Schematic diagrams of the seven possible ring-pair types. Each diagram is an accurate projection of the ring pairs generated by following the alogrithm of ref 16 and using the bond lengths and angles of the E1 and G1 rings of the observed structure. The E1 ring bond lengths and angles were averaged before use to make the ring twofold symmetric. The direction of projection is along the metal ion and the central nitrogen bond. See footnote 26 for an explanation of the symbols given in the figure.

Table IX. Angle between the Ring Planes of Various Ring-Pair Types[a]

Symbols[b]	Angle between mean planes, deg	Angle between ligand atom planes,[c] deg	Possible arrangement
EE(em)	155	147	Trans
EE(r)	120	120	Cis
EE(am)	85	87	Cis
EG(em)	161	166	Trans
EG(er)	111	101	Cis
EG(am)	78	74	Cis
EG(ar)	125	139	Cis, trans

[a] See footnote 27. [b] See Figure 4 for identification. [c] This is the angle between the M-N-N plane of the E ring and the M-N-N or M-N-O plane of the E or G ring that is fused to the first E ring. Here M is the metal ion.

found possible for each of the topological types of Figure 3: I, 4; II, 4; III, 4; IV, 8; V, 5; VI, 8; VII, 10. Each of these 43 isomers is optically active—including optical isomers, there are then 86 possible isomers for a sexadentate, octahedral complex of DTPA. Some of these will differ only slightly from others in shape. Not all of these isomers will have equal stability since intramolecular interatomic repulsions can be quite different among the different isomers. By way of illustration, the ten conformational isomers of type VII are shown in Figure 5. The observed structure is of type VIIa.

It is not possible at this time to formulate a definitive reasoning as to why, or indeed whether, the observed isomer is more stable than other possible types. It is, however, curious to note that all but types VI and VII require three contiguously fused chelate rings to lie at least approximately in one plane. Such an arrangement involves much strain,[18,24] especially for the trans types (types I–IV in which the two terminal nitrogens are trans to one another) since these require two highly ruffled E rings[16] to be in one plane. Types VI and VII are similar, the only difference being that the neutral carboxylic acid arm

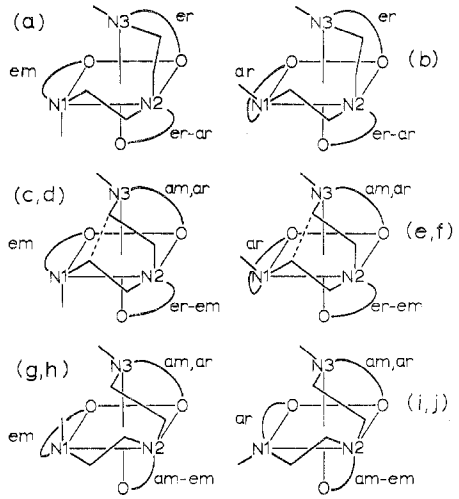

Figure 5. Schematic diagrams of the ten possible conformational isomers of the topological type VII. Conformation of the rings is indicated for E rings by the line joining the two nitrogen atoms of the ring and for G rings by explicit labels. The two labels given for the G2 ring refer to its type with respect to E1 and E2 rings, respectively. Only one diagram is given for two isomers when they differ only by the conformation of the G3 ring. Dotted lines indicate expected short contacts.

that carries the weakly bound axial oxygen ligand is from a terminal nitrogen in the former and from the middle nitrogen in the latter.

The observed conformational isomer may be selected from the 10 possibilities of topological type VII by making the following series of choices. (1) Choose the r-type E-ring pair. The only other alternative, the am type, is not as suitable because a short nonbonded contact exists in this type between a pair of methylene groups (indicated in Figure 5 by dotted lines). This feature was noted by Buckingham and his coworkers[29] in their study of the triethylenetetramine complexes. This choice amounts to rejecting types c–f. (2) Choose the G1 ring to be of the em type. The only other alternative is the ar type, of which the interplanar angle (Table IX) is not as suitable for a trans arrangement. This amounts to further rejecting types b, i, and j. (3) Of the remaining possibilities, choose the one in which the uncomplexed axial group of N_1 points to the less crowded side of the equatorial plane. This procedure then leads uniquely to the observed isomer a.

Description of the Conformation. We note first that the em-type arrangement of the E1 and G1 rings is similar to the E- and G-ring arrangement observed in $[Co^{III}EDTA]^-$, $Ni^{II}OH_2H_2EDTA$, and $Cu^{II}OH_2H_2EDTA$ complexes[18,24] (G ring in EDTA complexes is the glycinate ring that is roughly on the plane of the E ring). This arrangement is not as strain free as the E- and R-ring arrangement which also exists in these EDTA complexes. Significant compressions of the ring bond angles occur at the chelating nitrogen and oxygen atoms (Table V). The overall degrees of angular strain as measured by the ring angle sum (Table VIII) for these rings are comparable to 521, 515, and 514° observed for the E rings and 524, 525, and 527° for the G rings of the Co^{III}–, Ni^{II}–, and Cu^{II}–EDTA complexes[30] but much smaller than 538–539° for the R rings of these complexes. The Cu–O_1, Cu–N_1, and Cu–N_2 bond lengths (Table IV) are about equal to or longer than the corresponding[30] Cu–N (2.07 Å) and Cu–O (1.97 and 1.93 Å) distances in the dihydrogen copper(II) complex of EDTA and the corresponding Cu–N (2.07, 1.98 Å) and Cu–O (1.81, 1.95 Å) distances in the potassium salt of the Cu^{II}–EDTA complex.[31]

If the observed E1 and G1 ring arrangement is similar to the less favorable ring arrangement in the corresponding EDTA

complexes and hence not ideally suited for strong metal–ligand bonding, distortions in other rings in the structure are generally worse and appear to be at best equally unsuited for strong metal–ligand bond formation. In an r-type arrangement of two E rings, the angle between the two ring planes is expected to be much greater than 90° (Table IX). The observed angle between the mean planes of the two E rings and that between the two Cu–N–N planes are both 117°. This feature represents one of two most severe distortions of the coordination geometry of this structure. It puts the N_3 atoms away from the main axis and makes the Cu–N_3 bond weak and long. Such weakening of an axial bond is probably not a serious liability against the stability of a d^9 Cu(II) complex. Possibly more important are the distortions on the geometry of the five-membered rings that such lengthening of a metal–chelate bond necessarily produces.[16] One can indeed note that the angles CuN_3C_{10} and CuN_3C_{11} are about 10° short of the ideal tetrahedral angle (Table V) and that the N_3CuO_7 and N_2CuN_3 angles are 4–5° smaller than the corresponding angles in G1 and E1 rings. These unfavorable angular distortions are, however, partially compensated for by the favorable geometry around the ligand atoms N_2 and O_7. Thus the angles CuO_7C_{12} and CuN_2C_9 (Table V) are nearer the ideal trigonal and tetrahedral values than the corresponding angles in E1 and G1 rings. The ring angle sum for E2 and G3 rings (Table VIII) indicate that the overall angular strain in these rings is comparable to that of the E1 and G1 rings.

The large opening of the angle between the two E rings has a couple of other beneficial effects. First it eliminates the short contact that would otherwise exist between one of the groups attached to N_3 and the hydrogens of the methylene groups attached to N_1.[29] The shortest H···H contact distance in this region of the molecule is 2.59 Å, which occurs between two hydrogen atoms attached to C_{13} and C_1. Second, it helps put the O_7 atom in the plane of O_1–N_1–N_2. The angle subtended at the metal ion by the two ligand atoms of a G ring is always less than 90° (γ angle of ref 16). The angle for G3 ring (angle N_3CuO_7 in Table V) is especially small because of the long Cu–N_3 distance. This means that, if Cu–N_3 bond were normal to the O_1–N_1–N_2 plane, atom O_7 will hang considerably below (to the N_3 side of) this plane. The large opening of the angle between the Cu–N_1–N_2 and Cu–N_2–N_3 planes is, therefore, necessary in order to bring O_7 atom into the equatorial plane. We note parenthetically here that this movement of N_3 atom away from the main axis and toward the equatorial plane also necessitates an increase (from the ideal 90°) in the angle between the E2 and G3 ring planes. This increase is nicely accommodated by the er-type arrangement of the G3 ring with respect to the E2 ring (Table IX). The observed values for the angles between the mean planes and between the ligand atom planes of these two rings are 110 and 111°, respectively. The end result of all these movements and adjustments is the formation of the relatively strong Cu–O_7 bond in spite of the long Cu–N_3 bond and of the large angular strain of the rings.

The other major distortion of the coordination polyhedron involves the formation of the G2 ring and of the Cu–O_5 bond. The G2 ring is er with respect to E1 and ar with respect to E2. The expected angle between the ligand atom planes of G2 and E1 is much greater than the ideal value of 90° while that between G2 and E2 is much smaller than the ideal value of 180° (Table IX). In order to bring these angles closer to the ideal values, the G2 ring and the carbon atoms attached to N_2 are rotated around the Cu–N_2 bond clockwise in the view of Figure 1. This rotation can be detected from the position of the carbon atoms in the E rings. The two carbon atoms in an E ring should normally be displaced to either side of the Cu–N–N plane by the same amount. However, if a clockwise rotation of the kind described above occurs, the carbon atom attached to N_2 will be closer to the Cu–N–N plane than the other carbon atom of the ring. Indeed it is observed that the N_2-bound C_6 and C_9 atoms are only 0.24 and 0.18 Å off the Cu–N–N plane of their respective rings while the atoms C_5 and C_{10} are 0.43 and 0.50 Å off these planes. The observed angle between the Cu–N_1–N_2 and Cu–N_2–O_5 planes after this rotation is 90° but that between the Cu–N_2–N_3 and Cu–N_2–O_5 planes is 153°. Thus the distortion in the coordination geometry is not completely removed with the result that the Cu–O_5 bond is considerably off from the main axis and is extremely long. The large deviation of the CuO_5C_8 angle from the ideal trigonal angle (Table V), the large ruffling of the ring as indicated by the small ring angle sum of 520°, and the small N_2CuO_5 angle are all necessary consequences of the long Cu–O_5 bond length.

Registry No. $H_3CuDTPA \cdot H_2O$, 54244-37-0.

Supplementary Material Available. Tables I, IIa, and IIb will appear following these pages in the microfilm edition of this volume of the journal. Table I contains a list of the calculated and observed structure factors, Table IIa a list of the anisotropic thermal parameters for all nonhydrogen atoms, and Table IIb a list of the positional and isotropic thermal parameters for the carbon-attached hydrogen atoms. Photocopies of the supplementary material from this paper only or microfiche (105 × 148 mm, 24× reduction, negatives) containing all of the supplementary material for the papers in this issue may be obtained from the Journals Department, American Chemical Society, 1155 16th St., N.W., Washington, D.C. 20036. Remit check or money order for $4.50 for photocopy or $2.50 for microfiche, referring to code number AIC40697B.

References and Notes

(1) L. G. Sillén and A. E. Martell, *Chem. Soc., Spec. Publ.*, **No. 17** (1964).
(2) (a) S. Chaberek, A. E. Frost, M. A. Doran, and N. J. Bicknell, *J. Inorg. Nucl. Chem.*, **11**, 184 (1959); (b) R. Harder and S. Chaberek, *ibid.*, **11**, 197 (1959); (c) J. Vandegaer, S. Chaberek, and A. E. Frost, *ibid.*, **11**, 210 (1959).
(3) R. E. Sievers and J. C. Bailar, Jr., *Inorg. Chem.*, **1**, 174 (1962).
(4) B. B. Smith and R. H. Betts, *J. Amer. Chem. Soc.*, **91**, 7749 (1969).
(5) A. R. Fried, Jr., and A. E. Martell, *J. Amer. Chem. Soc.*, **93**, 4695 (1971).
(6) J. J. Stezowski, R. Countryman, M. O'D. Julian, V. W. Day, R. E. Hughes, and J. L. Hoard, paper presented at the 14th International Conference on Coordination Chemistry, Toronto, Canada, 1972.
(7) R. Seccombe and B. Lee, paper presented at the 8th Midwest Regional Meeting of the American Chemical Society, Columbia, Mo., 1972.
(8) V. V. Fomenko, T. N. Polynova, M. A. Porai-Koshits, G. L. Varlamova, and N. I. Pechurova, *Zh. Strukt. Khim.*, **14**, 571 (1973).
(9) "$P\bar{1}$ Operations Manual," Syntex Analytical Instruments, Cupertino, Calif., 1972.
(10) G. Friedlander and J. W. Kennedy in "Introduction to Radiochemistry," Wiley, New York, N.Y., 1949, p 214.
(11) P. W. R. Corfield, R. J. Doedens, and J. A. Ibers, *Inorg. Chem.*, **6**, 197 (1967).
(12) A. Zalkin's FORDAP for the Fourier summation, W. Busing, K. Martin, and H. Levy's ORFLS and ORFFE-II for the least-squares and function and error calculations, and C. K. Johnson's ORTEP-II for the molecular structure drawing.
(13) D. T. Cromer and J. B. Mann, *Acta Crystallogr., Sect. A*, **24**, 321 (1968).
(14) J. A. Ibers, "International Tables for X-Ray Crystallography," Vol. III, Kynoch Press, Birmingham, England, 1962, Tables 3.3.1A and 3.3.2C.
(15) Supplementary material.
(16) B. Lee, *Inorg. Chem.*, **11**, 1072 (1972), and other references cited therein.
(17) IUPAC Commission on Nomenclature in Inorganic Chemistry, *Inorg. Chem.*, **9**, 1 (1970).
(18) H. A. Weakliem and J. L. Hoard, *J. Amer. Chem. Soc.*, **81**, 549 (1959).
(19) J. D. Dunitz, *Tetrahedron*, **28**, 5459 (1972).
(20) F. A. Cotton and G. Wilkinson, "Advanced Inorganic Chemistry," 2nd ed, Wiley, New York, N.Y., 1966, p 683.
(21) E. J. Durham and D. P. Ryskiewich, *J. Amer. Chem. Soc.*, **80**, 4812 (1958).
(22) G. L. Blackmer and J. L. Sudmeier, *Inorg. Chem.*, **10**, 2019 (1971).
(23) These are the logarithms of the equilibrium constant for the reaction whereby the complex is formed from the metal ion and the chelating agent in aqueous solution.
(24) G. S. Smith and J. L. Hoard, *J. Amer. Chem. Soc.*, **81**, 556 (1959); F. S. Stephens, *J. Chem. Soc. A*, 1723 (1969).
(25) R. S. Cahn, C. Ingold, and V. Prelog, *Angew. Chem., Int. Ed. Engl.*, **5**, 385 (1966).
(26) The names of the ring-pair types given in Figure 4 contain symbols in parentheses that have the following meaning. Choose as reference the E ring for an EG pair or either one of the two E rings for an EE pair. The letters e and a indicate the mode of attachment of the E or G ring to this reference ring, e for equatorial and a for axial. The letters m

and r indicate the relative conformation of the two rings of the pair, m if the two rings are both δ or both λ and r if one is δ while the other is λ.
(27) The geometry of the five-membered rings used for this computation was obtained following the algorithm presented earlier[16] and using the bond length and angle data of the E1 and G1 rings of the observed $H_3Cu^{II}DTPA$ complex. Since the bond lengths and angles of a five-membered chelate ring can vary considerably, the numbers given should be used with caution. They are meant to give gross, qualitative tendencies rather than exact, quantitative measures.
(28) With small metal ions, the axial G rings can be quite flat. In this case, the distinction between the ar and am types disappears, the interplanar angle will be intermediate between those for the ar and am types, and the preferred configuration will be cis.
(29) D. A. Buckingham, I. E. Maxwell, A. M. Sargeson, and M. R. Snow, *J. Amer. Chem. Soc.*, **92**, 3617 (1970).
(30) The comparison to the Cu^{II}–EDTA structure is complicated by the fact that the E and G rings in this structure span axial ligands, *i.e.*, the terminal ligands of this ring pair form long bonds to the copper ion under the possible influence of the Jahn–Teller effect.[24] In contrast, the E1 and G1 rings of the present DTPA structure lie on the equatorial plane and their ligand atoms form normal bonds to the copper ion. We compare the ring angle sums of the E1 and G1 rings of the DTPA structure to those of the E and G rings of the EDTA structure, but the bond lengths $Cu-O_1$, $Cu-N_1$, and $Cu-N_2$ of the DTPA structure are compared to the equatorial bonds of the R rings of the EDTA structure.
(31) N. V. Novozhilova, T. N. Polynova, M. N. Porai-Koshits, and L. I. Martynenko, *Zh. Strukt. Khim.*, **8**, 553 (1967).

Contribution from the Department of Chemistry,
University of Melbourne, Parkville, 3052, Melbourne, Victoria, Australia

Kinetics and Stereochemistry of Solvolysis of *cis*- and *trans*-Dibromo- and Bromochlorobis(ethylenediamine)chromium(III) Complexes in Dipolar Aprotic Solvents

W. G. JACKSON* and W. W. FEE

Received April 22, 1974 AIC40261W

The primary solvolysis of bromide ion from each of the *cis*- and *trans*-dibromobis(ethylenediamine)chromium(III) cations occurs completely and with steric retention in dimethylformamide. Both cis and trans isomers of the product bromo(dimethylformamide) complex have been isolated. The rates and equilibria have been studied and were found not to be significantly dependent upon the concentration of added bromide ion, despite considerable ion pairing of the ground-state reactants (established independently). Activation parameters have been measured. For the bromochloro isomers in dimethylformamide and dimethyl sulfoxide, solvolysis of bromide is much faster than that of chloride and is measurably reversible. The reactions in both solvents are quite analogous to those of the dibromo complexes, but they yield exclusively the isomeric chloro(solvento) complexes as products in these cases. Again, both the cis and trans isomers of the product complexes $Cr(en)_2(DMF)Cl^{2+}$ and $Cr(en)_2(DMSO)Cl^{2+}$ have been isolated. For these and related reactions, cis:trans and bromide:chloride rate ratios and the qualitative effect of solvent transfer on these are shown to be consistent with a common dissociative mechanism.

Introduction

The present work was initiated as part of a more general program concerned with chromium(III) substitution reactions in relation to their well-studied cobalt(III) analogs. This and subsequent publications will describe the kinetics and stereochemistry of bis(ethylenediamine)- and tetraamminechromium(III) complexes in dipolar aprotic media. Watts, *et al.*, have recently reported on the reactions of the dichlorobis(ethylenediamine)chromium(III) complexes in dimethylformamide (DMF)[1] and dimethyl sulfoxide (DMSO)[2,3] and the analogous dibromo cations in DMSO.[4] Moreover, an independent study of the important ion-pairing process for a wider range of such chromium(III) complexes in dipolar aprotic media has been reported.[5] In this paper we consider the primary solvolysis reactions of the *cis*- and *trans*-$Cr(en)_2Br_2^+$ ions in DMF and *cis*- and *trans*-$Cr(en)_2ClBr^+$ ions in both DMF and DMSO. Thus this work now completes the dichloro, dibromo, and bromochloro complex systems in these two solvents. The directly analogous cobalt(III) reactions have been studied.[8-12]

The reactions reported here for the solvolyses of the relatively labile bromide leaving group were expected to be uncomplicated by chromium–nitrogen cleavage side reactions which are often prevalent in aqueous and other nonaqueous Cr(III) systems.[6] The studies of the reactions of the *cis*- and *trans*-halo(solvento) and bis(solvento) complexes which complete this research are appropriately treated elsewhere[7] because parallel amine dissociation reactions are important there.

* Author to whom all correspondence should be addressed at the University Chemical Laboratory, Cambridge University, Cambridge, CB2 1EW, England.

Experimental Section

Preparation of Complexes. *cis*- and *trans*-$[Cr(en)_2ClBr]Br\cdot H_2O$ and *cis*- and *trans*-$[Cr(en)_2ClBr]ClO_4$ were synthesized as described previously.[13]

A new, easier, and more convenient synthesis of *trans*-$Cr(en)_2ClBr^+$ is as follows. A hot, saturated solution (pink-red) of *trans*-$[Cr(en)_2(OH_2)Cl]Br_2$[13] in tetramethylene sulfone readily turns green at steam bath temperatures and then deposits fine green crystals of *trans*-$[Cr(en)_2ClBr]Br$. After complete reaction (approximately 10 min) acetone was added to complete crystallization. The product was collected and washed with acetone–water (1:1) and finally with ether. The yield is essentially quantitative. Deep green-blue needles of the monohydrate were obtained by recrystallization.[13] The perchlorate by metathesis in water (sodium perchlorate) was recrystallized from cold DMF by the slow addition of aqueous sodium perchlorate. *Anal.* Calcd for $[Cr(en)_2ClBr]Br\cdot H_2O$: C, 12.4; H, 4.7; N, 14.5; Br, 41.5; Cl, 9.2. Found (cis): C, 12.3; H, 4.8; N, 14.5; Br, 41.7; Cl, 8.6. Found (trans): C, 12.1; H, 4.7; N, 14.2; Br, 42.2; Cl, 9.0. Calcd for $[Cr(en)_2ClBr]ClO_4$: Cr, 13.4; C, 12.4; H, 4.1; N, 14.5; Br, 20.6; Cl, 18.3. Found (cis): Cr, 13.4; Br, 20.7; Cl, 18.1. Found (trans): Cr, 13.3; C, 12.3; H, 3.9; N, 14.0; Br, 20.8; Cl, 18.3.

Caution! Perchlorates are potentially explosive. For example, in our hands *cis*-$[Cr(en)_2Br_2]ClO_4$ has exploded violently on heating rapidly to 130°. Room-temperature drying is recommended.

cis-$[Cr(en)_2Cl_2]Cl\cdot H_2O$,[14,15] recrystallized from water–hydrochloric acid (10 *M*)–ethanol (1:1:1), was converted to the bromide ($\cdot H_2O$) and then to *cis*-$[Cr(en)_2Br_2]Br\cdot H_2O$ by a known method[16] modified as described now. An aquated *cis*-$Cr(en)_2Cl_2^+$ solution[16] ($Cr(en)_2(OH)_2)_2^{3+}$) was taken to dryness three times with hydrobromic acid (48%) to yield completely chloride free $[Cr(en)_2Br_2]Br$. Very rapid evaporation is essential (<50°; rotary evaporation). Prepared in this way, traces of trans isomer are produced which are readily removed by recrystallization as the bromide salt from ice-cold DMF solution by the addition of cold aqueous sodium bromide. Fine shiny